International Journal of Fracture **94:** 285–297, 1998.

Studies on elastic coupling parameters of fracture modes in orthotropic materials

A.V. KRISHNA MURTY* and A. NAGAMANI**
Department of Aerospace Engineering, Indian Institute of Science, Bangalore–560 012, India.
e-mail: avk@aero.iisc.ernet.in

Received 29 January 1998; accepted in revised form 5 October 1998

Abstract. The characterisation of cracks is usually done using the well known three basic fracture modes, namely opening, shearing and tearing modes. In isotropic materials these modes are uncoupled and provide a convenient way to define the fracture parameters. It is well known that these fracture modes are coupled in anisotropic materials. In the case of orthotropic materials also, coupling exists between the fracture modes, unless the crack plane coincides with one of the axes of orthotropy. The strength of coupling depends upon the orientation of the axes of orthotropy with respect to the crack plane and so the energy release rate components associated with each of the modes vary with crack orientation. The variation, of these energy release rate components with the crack orientation with respect to orthotropic axes, is analyzed in this paper. Results indicate that in addition to the orthotropic planes there exist other planes with reference to which fracture modes are uncoupled.

Notation

E_L and E_T	Longitudinal and transverse moduli
$F_i (i = x, y)$	Nodal forces
G	Total strain energy release rate
G_{I}, G_{II} and G_{III}	Strain energy release rates associated with opening, shearing and tearing modes of fracture respectively
G_{LT}	Shear modulus
a	Crack length
g_{ij}	Strain energy release rate components
$\hat{u}_{ij}$ and $\hat{u}'_{ij}$	Displacement parameters
$\delta\hat{u}_{ij}$	Relative displacement in the j-direction ($i = 1, 2, 3$)
Δa	Small increment of crack
ν_{LT}	Poisson's ratio in LT direction
$\sigma_i (i = 1, 2, 3)$	Stress component

1. Introduction

In isotropic materials, the fracture modes are uncoupled and so the fracture toughness of each of the modes, may be determined by designing specimens/experimental conditions, representing only one of the fracture modes at a time. The experimentally determined material constants are then used to study the more general case of mixed mode of fracture. However, in the case

* Professor
** M.E. student

of orthotropic materials, the fracture modes are usually coupled except when the crack plane coincides with a plane containing orthotropic axes.

The behavior of a crack located in an orthotropic plane may be expected to be governed by three parameters, representing the strain energy release rate in opening, shearing and tearing of the crack. Since there are three such planes, a total of nine basic material parameters may be expected to influence the behavior of a general crack in the orthotropic material. In order to make coupling parameters to be available explicitly, the strain energy release rate can be expressed as a sum of nine components–with three of them representing direct action of opening, shearing and tearing and the other six parameters representing the coupling effect between modes. The availability of coupling parameters may be relevant in the case of interface fracture also as in this case the fracture modes are usually coupled. The mode coupling conditions at the tip of the crack in orthotropic material introduces mode mixity and hence cause crack kinking. The study of the variation of the strain energy release rate components is an important step in understanding the kinking phenomenon. It may be noted here that the mode mixity arises primarily due to two reasons, namely due to (a) applied loading as in the case of isotropic materials and (b) coupling of fracture modes or a combination of both. The availability of coupling Strain Energy Release Rate (SERR) parameters is expected to aid the understanding the effect of elastic coupling of fracture modes on fracture behavior of orthotropic materials and to formulate generalised mixed mode crack growth criteria for cracking of orthotropic material treating coupling energy terms as additional parameters.

Analysis of plane cracks and crack kinking in homogeneous, isotropic elastic solids has been dealt extensively in the literature (Hayashi and Nemat-Nasser, 1981; He and Hutchinson, 1989; He et al., 1991). Analysis of plane cracks aligned with principal axes of orthotropy and kinked cracks in a homogeneous, orthotropic elastic solids has been discussed by Hutchinson and Suo (1991). Traditionally, the behavior of cracks in an orthotropic medium has been viewed as an extension of the behavior of cracks in a homogeneous medium. Techniques for computing stress intensity factors are available in the literature for plane and slant cracks in orthotropic and anisotropic bodies by extending methods originally developed for isotropic materials (Sih et al., 1965; Bowie and Freese, 1972; Gandhi, 1972; Kaya and Erdogan, 1980; Lee, 1990; Sollero and Aliabadi, 1993). Strain energy release rates associated with opening, shearing and tearing modes of fracture, namely G_{I}, G_{II} and G_{III} are used to characterize the crack behavior. In contrast to the isotropic case, fracture modes in orthotropic medium are coupled as mentioned earlier. In this paper, strain energy release rate components representing the coupling between the basic fracture modes are estimated and their variation with respect to axes of orthotropy has been investigated. The present study is intended as a step towards more general studies on crack growth behaviour in orthotropic medium to explore the usefulness of the SERR coupling parameters in formulating mixed-mode crack growth criteria for crack growth.

2. SERR Expression for orthotropic materials

Figure 1 shows a typical orthotropic material containing a general crack, with the crack plane located at an angle with the axis of the orthotropy. Let (x, y, z) represent a crack tip coordinate system, such that the crack faces lie in the (x, y) plane. During the growth of the crack strain energy is released. Let the crack be extended by a small increment Δa. The energy released

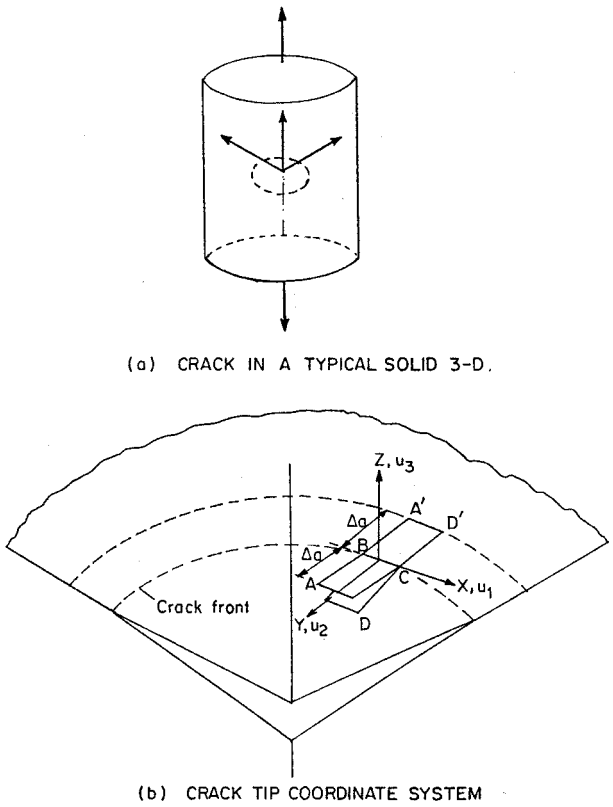

Figure 1. (a) Crack in a typical solid 3-D. (b) Crack tip coordinate system.

during the extension of the crack is the same as that required to close the crack back to its original position.

Following the virtual crack closure integral (Rybicki and Kanninen, 1977), the strain energy release rate G can be expressed as

$$G = \frac{1}{2.BC.BA} \int_{x^B}^{x^C} \int_{y^B}^{y^A} \sigma_j(x, (y - \Delta a)) \delta u_j(x, y)\, \mathrm{d}x\, \mathrm{d}y \quad j = 1, 2, 3, \tag{1}$$

where $\sigma_j(x, (y - \Delta a))$ represents the stress distribution ahead of the crack tip and $\delta u_j(x, y)$ represents the relative displacements between the two crack surfaces. Note that $\sigma_1 = \sigma_{xz}$, $\sigma_2 = \sigma_{yz}$ and $\sigma_3 = \sigma_{zz}$.

δu_j consists of three components each one, arising due to one of the three stress components σ_i as

$$\delta u_j = \delta \hat{u}_{1j} + \delta \hat{u}_{2j} + \delta \hat{u}_{3j}, \tag{2}$$

where $\delta \hat{u}_{ij}$ represents the relative displacement in the j-direction due to stress component $\sigma_i (i = 1, 2, 3)$ applied at the corresponding point on the crack tip as shown in Figure 2.

Using (1) and (2) the expression for total strain energy release rate G is

$$G = \sum_{i=1}^{3} \sum_{j=1}^{3} g_{ij}, \tag{3}$$

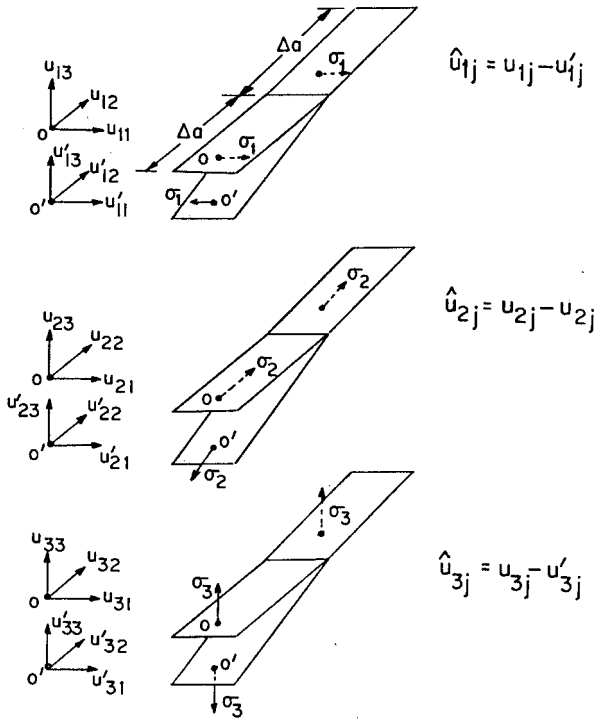

Figure 2. Stresses and displacements involved in SERR expression.

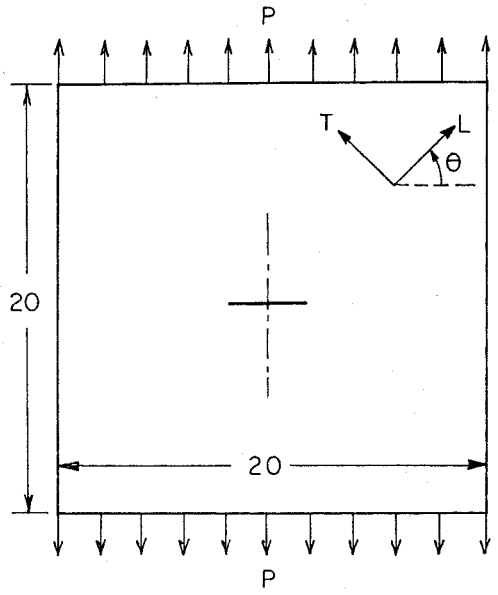

Figure 3. A typical crack in an orthotropic plate under extension.

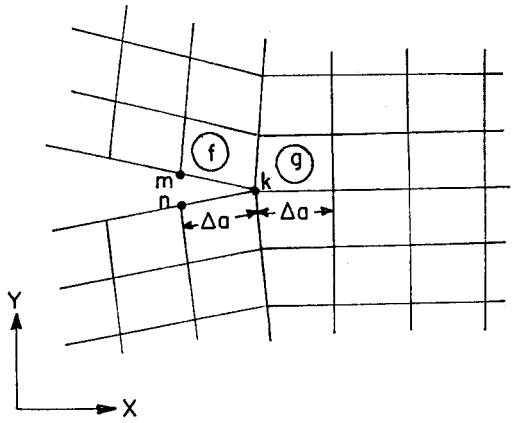

Figure 4. A typical finite element mesh near crack-tip.

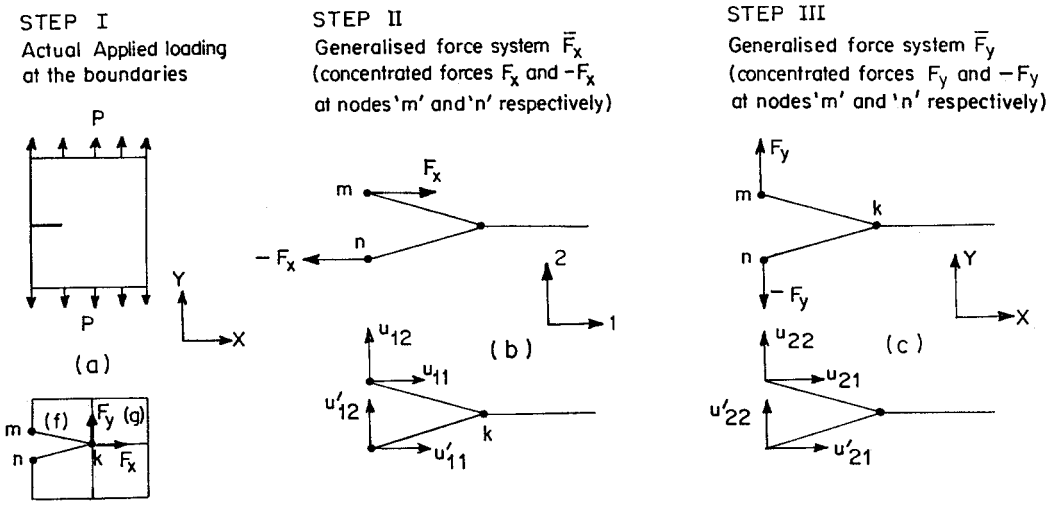

Figure 5. Details of the three step computations.

where

$$g_{ij} = \frac{1}{2.BC.BA} \int_{x^B}^{x^C} \int_{y^B}^{y^A} \sigma_i(x, (y - \Delta a))\ \ \delta\hat{u}_{ij}(x, y)\, \mathrm{d}x\, \mathrm{d}y \quad \text{(no sum on } i\text{)} \tag{4}$$

It may be noted that the nonzero coupling parameters $g_{ij}(i \neq j)$ are characteristic of cracks in orthotropic medium. In case of cracks in isotropic media the coupling terms are zero and the conventional G_{III}, G_{II} and G_{I} energy release rates respectively are $G_{\mathrm{I}} = \sum g_{3j}$, $G_{\mathrm{II}} = \sum g_{2j}$, $G_{\mathrm{III}} = \sum g_{1j}$

An essential step in the definition of g_{ij} is to recognize the coupling of fracture modes in producing of the relative displacements of the crack surfaces ($\delta\hat{u}_{ij}$). In references Eggers also introduced the coupling effect in the two-dimensional case, as applicable to the study of delaminations. Generalisation of the concept to the 3-D case has been discussed in Krishna Murty et al. (1994) also.

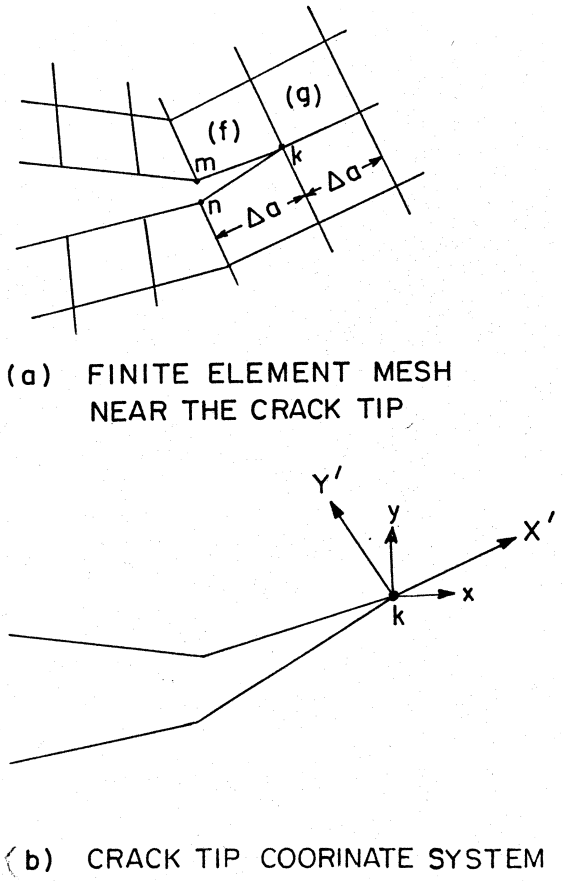

Figure 6. The kinked crack: geometry and coordinate system. (a) Finite element mesh near the crack tip. (b) Crack tip coordinate system.

3. 2-D Case and computation of SERR components

In what follows we consider the 2-D case for the study of coupling parameters in SERR. Figure 3 shows a typical orthotropic 2-D problem with a central crack modelled using finite elements. In the present study, quadrilateral element is used for simulation. The finite element mesh near the crack tip is shown in Figure 4.

The strain energy release rate components g_{ij} for a plane crack in a 2-D case can be defined as

$$g_{ij} = \frac{1}{2\Delta a} F_i(\hat{u}_{ij}^m - \hat{u}_{ij}^n), \tag{5}$$

where $(i, j = x, y)$.

The displacement parameters $\hat{u}_{ij}^m$ and $\hat{u}_{ij}^n$ in (5) are defined as the relative displacement in j-axis due to a generalized force in the i-direction applied at node 'm' and node 'n' respectively (see Figure 4). Figure 5 describes the steps used.

Step 1. Obtain nodal forces $F_i(i = x, y)$ as contributed from elements 'f' and 'g' at node 'k' for the case of applied uniform loads at the boundaries. (see Figure 5a).

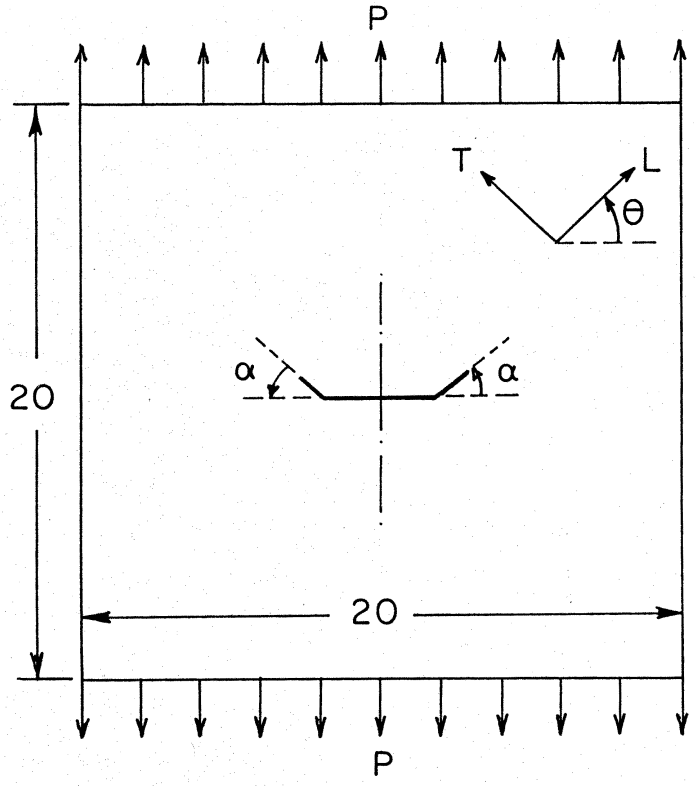

Figure 7. Central kinked crack in an orthotropic plate under extension.

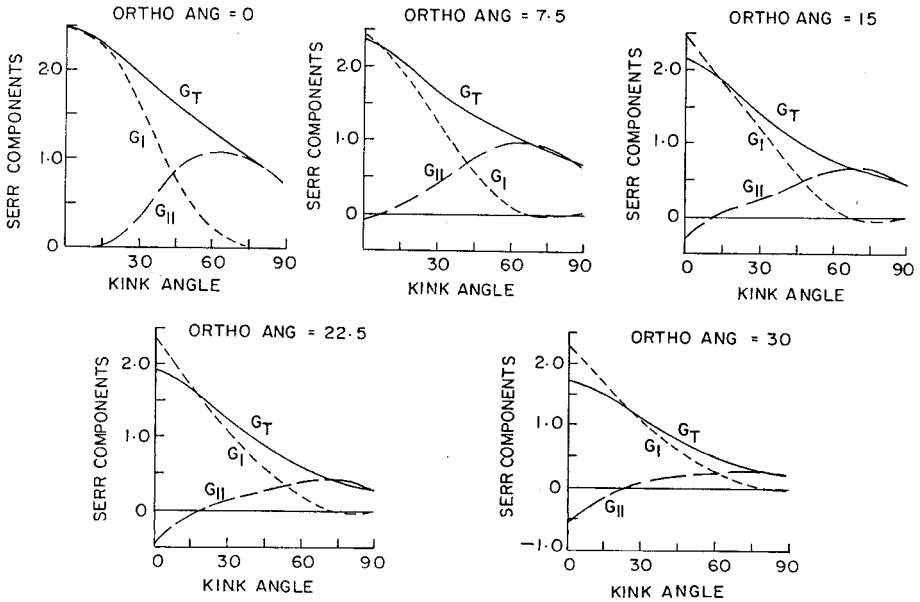

Figure 8a. First simulation (10,400 elements).

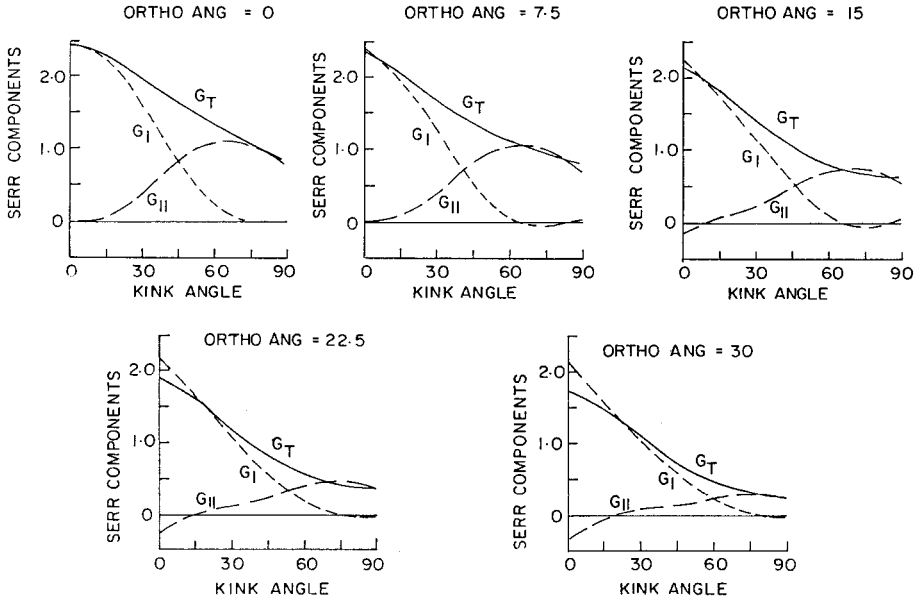

Figure 8b. Second simulation (15,600 elements).

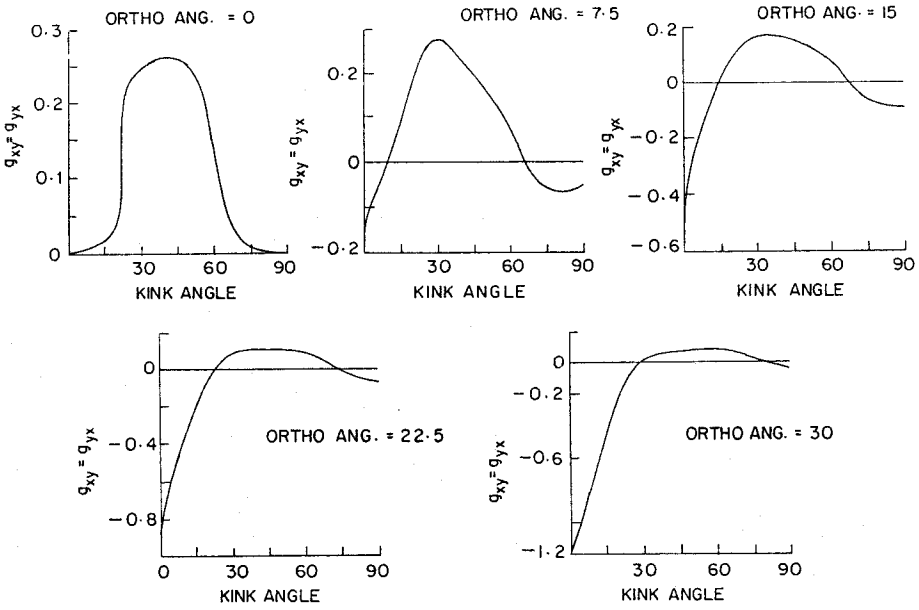

Figure 9a. Variation of g_{xy}.

Step 2. Apply generalised force system $\bar{F}_x$, consisting of concentrated forces F_x and $-F_x$ at nodes 'm' and 'n' respectively to obtain u_{1j} and u'_{1j}, $j = 1, 2$. (see Figure 5b).

Step 3. Similarly apply the generalised force system $\bar{F}_y$, consisting of concentrated forces F_y and $-F_y$ at nodes 'm' and 'n' respectively and obtain displacements u_{2j} and u'_{2j}, where $j = 1, 2$. (see Figure 5c).

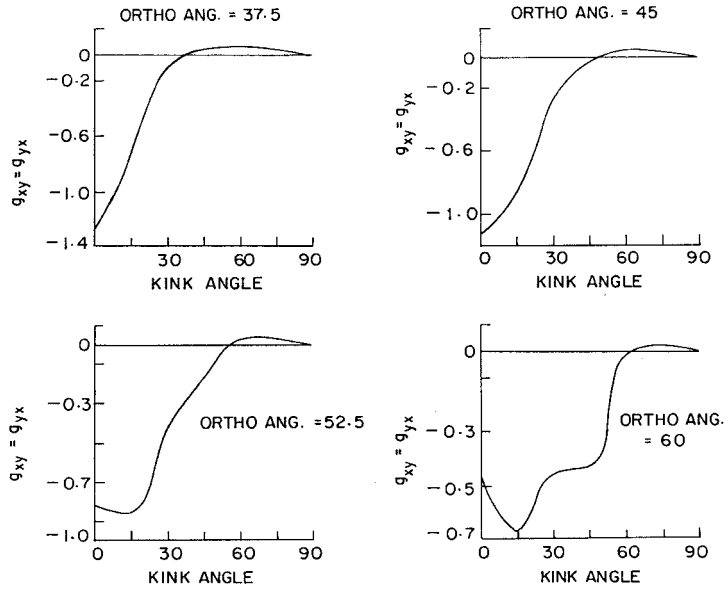

Figure 9b. Variation of g_{xy}.

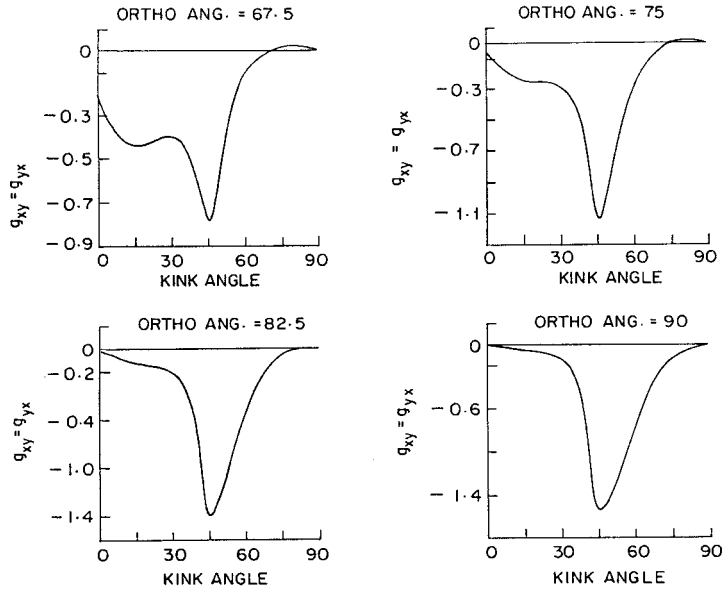

Figure 9c. Variation of g_{xy}.

Using these estimates of nodal forces and displacements in (5), components for g_{ij} may be evaluated. The relative magnitude of the coupling in g_{ij} gives a measure of the degree of anisotropy.

It should also be noted that conventional strain energy release rates G_{I} and G_{II} are given by $G_{\mathrm{I}} = g_{yy} + g_{yx}$ and $G_{\mathrm{II}} = g_{xx} + g_{xy}$.

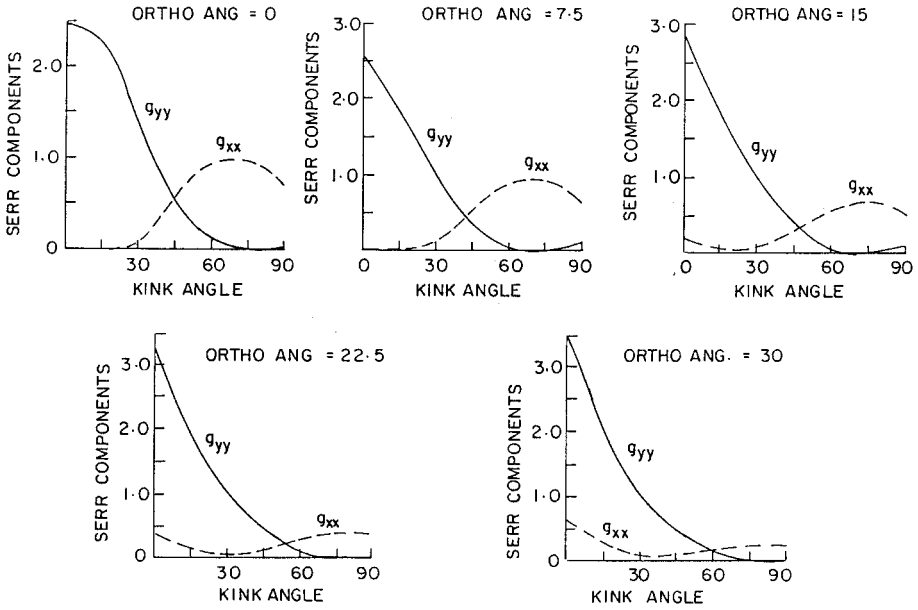

Figure 10a. Variation of g_{xx} and g_{yy}.

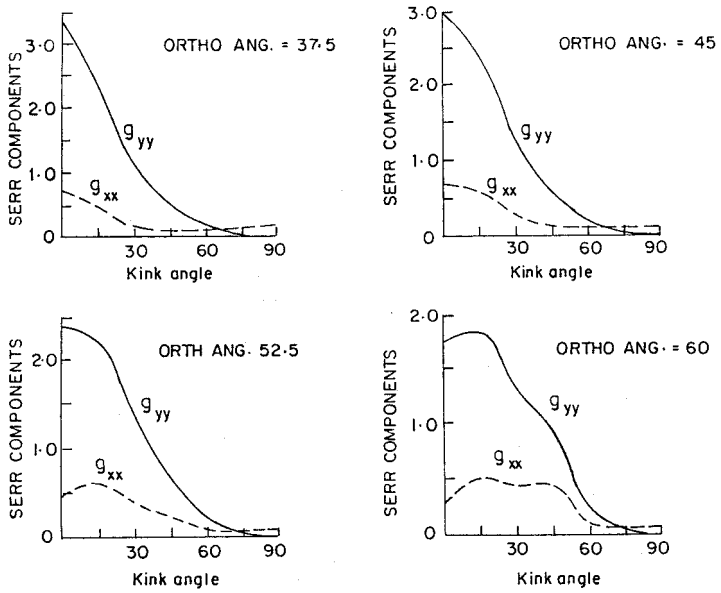

Figure 10b. Variation of g_{xx} and g_{yy}.

4. SERR Components for a kinked crack

To bring out the variation of the coupling components of SERR with crack orientation a kinked crack configuration shown in Figure 6 has been considered. A finite element analysis of the panel with kinked crack configuration gives the forces and displacements in global co-ordinate

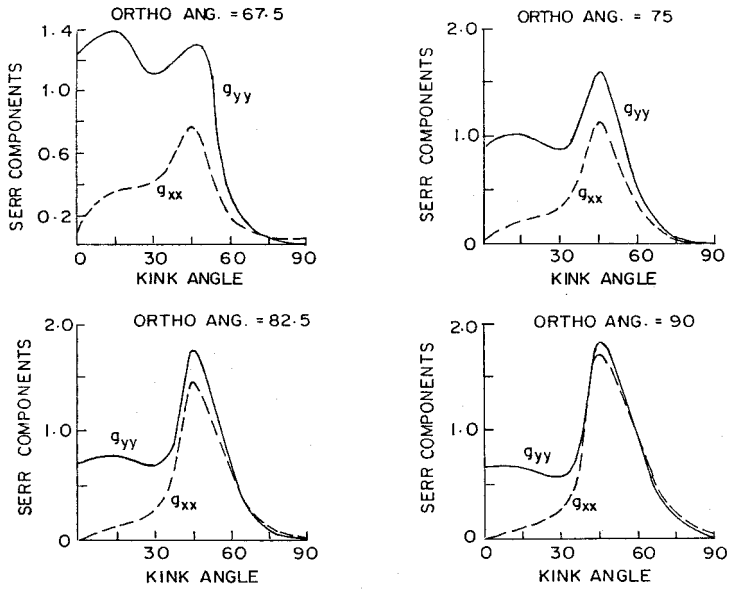

Figure 10c. Variation of g_{xx} and g_{yy}.

system (x, y). The forces and displacements obtained from the analysis are transformed for different kink axes (x', y') as follows. (also see Figure 6)

$$\begin{aligned} F_x^{'} &= F_x \cos\alpha + F_y \sin\alpha \\ F_y^{'} &= F_y \cos\alpha - F_x \sin\alpha. \end{aligned} \tag{6}$$

Similarly

$$\begin{aligned} u_x^{'} &= u_x \cos\alpha + u_y \sin\alpha \\ u_y^{'} &= u_y \cos\alpha - u_x \sin\alpha, \end{aligned} \tag{7}$$

where F_x, F_y, u_x, u_y are forces and displacements corresponding global coordinate system and $F_x^{'}, F_y^{'}, u_x^{'}, u_y^{'}$ are forces and displacements along with respect to $(X^{'}, Y^{'})$ system. Following (5) the strain energy release rate components $g_{ij}^{'}$ for a kinked crack in a 2-D case as a function of crack angle α can be defined as

$$g_{ij}^{'}(\alpha) = \frac{1}{2\Delta a} F_i^{'}(\hat{u}_{ij}^{m'} - \hat{u}_{ij}^{n'}), \tag{8}$$

where $F_i^{'}$, $\hat{u}_{ij}^{m'}$ and $\hat{u}_{ij}^{n'}$ are transformed forces and displacements as described in (6) and (7) respectively. Correspondingly

$$G_{\mathrm{I}}^{'} = g_{yy}^{'} + g_{yx}^{'}, \qquad G_{\mathrm{II}} = g_{xx}^{'} + g_{xy}^{'} \quad \text{and} \quad G = G_{\mathrm{I}} + G_{\mathrm{II}}. \tag{9}$$

5. Results and discussion

The orthotropic plate with the central cracks subjected to uniform stresses is considered for numerical study. The size of the crack is considered to be small compared to the width of the

plate. For numerical investigation, the material properties are taken as $E_L = 20.0$, $E_T = 1.0$, $\nu_{LT} = 0.3$ and $G_{LT} = 0.8$. In typical cases, the results obtained by considering half plate finite element simulation are compared with full simulation to examine the adequacy of the half plate simulation for generating numerical data. In view of close agreement, half plate simulation is adopted for numerical study. Finite element analysis using the Crack Closure Integral (CCI) technique has been used to calculate the SERR components.

Various combinations of the kink angle with orthotropic angle of the material are examined (Figure 7). The kink angle is varied from 0 to 90 degrees in steps of 15 degrees and the orthotropic angle from 0 to 90 degrees in steps of 7.5 degrees. Two finite element simulations are considered. The first one has 10,400 four noded plane stress elements with the ratio $\Delta a/a$ as 0.1. The main crack is divided equally into 10 parts by putting 11 nodes. There are no nodes in the kinked crack except at the crack-tip. In the second simulation the mesh is refined to 15,600 four noded plane stress elements reducing $\Delta a/a$ as 0.02. The main crack is divided into 50 portions. The kinked crack is divided equally into 5 portions reducing the distance between two adjacent nodes to 0.02 units. The mesh generation and the analysis is done using NISA-II general purpose finite element software. Results for both cases are presented in typical cases (Figures 8a and 8b). In view of good comparison, the second mesh is used to generate all the data.

The expression for g'_{ij}, G'_{I} and G'_{II} are given by (8) and (9). The variation of strain energy release rate components for various crack kink angles α with the orthotropic angle θ is presented in Figures 9(a–c) and Figures 10(a–c).

Figures 9(a–c), show the variation of elastic fracture mode coupling parameters g_{xy} for various orthotropic angle and kink angle. The location of the plane where the parameter g_{xy} becomes zero indicates that no coupling exists between the fracture modes. Also it is to be noted that when the kink angle coincides with the orthotropic angle, the coupling parameter g_{xy} vanishes. Interestingly, crack planes (kink angles) for which $g_{xy} = 0$, other than those corresponding to orthotropic planes, may be noted and it requires careful further studies.

6. Conclusion

The variation of strain energy release rate components at the crack tip in an orthotropic plate has been investigated. The SERR components, representative of elastic coupling have been identified and numerically estimated. It is observed that the coupling energy terms g_{xy} and g_{yx} are always equal and they are zero when the crack lies along one of the principal planes of orthotropy. In addition, there exists other crack kinking planes in which coupling energy terms are zero.

Acknowledgements

The authors had very useful discussion with J.N. Reddy, Hans Eggers, K.N. Raju and H.K. Harikumar at various stages of this work. The help of B. Syam Sunder and G. Narayana Naik and M. Kumar in preparing the manuscript is gratefully acknowledged.

References

Bowie, O.L. and Freese, C.E. (1972). Central crack in rectangular sheet with rectilinear anisotropy. *International Journal of Fracture Mechanics* **6**, 245–251.

Eggers, H. (1988). Analysis of delamination growth. *Proceedings of International Conference 'Spacecraft Structures and Material Testing' Noordwijk*, The Netherlands, ESA SP-289.

Gandhi, K.R. (1972). Analysis of an inclined crack centrally placed in an orthotropic rectangular plate. *Journal of Strain Analysis* **7**, 157–162.

Hayashi, K. and Nemat-Nasser, S. (1981). Energy-Release rate and crack kinking under combined loading. *Journal of Applied Mechanics* **48**, 520–524.

He, M.Y. and Hutchinson, J.W. (1989). Kinking of a crack out of an interface. *Journal of Applied Mechanics* **56**, 270–278.

He, M.Y., Barlett, A., Evans, A.G. and Hutchinson, J.W. (1991). Kinking of a crack out of an interface: Role of in-plane stress. *Journal American Ceramic Society* **74**, 767–771.

Hutchinson, J.W. and Suo, Z. (1991). *Advances in Applied Mechanics*, Academic press, **29**, 63–191.

Kaya, A.C. and Erdogan, F. (1980). Stress intensity factor and crack opening displacement in an orthotropic strip. *International Journal of Fracture* **16**, 171–190.

Krishna Murty, A.V., Reddy, J.N. and Harikumar, H.K. (1994). A new strain energy release rate concept for interfacial cracks. *Proceedings of the Indo-German Workshop* 62–67.

Lee, J.C. (1990). Analysis of a fiber bridged crack near a free surface in ceramic matrix composites. *Engineering of Fracture Mechanics* **37**, 209–219.

Rybicki, E.F. and Kanninen, M.F. (1977). A finite element calculation of stress intensity factor by the modified crack closure integral. *Engineering of Fracture Mechanics* **9**, 931–938.

Sih, G.C., Paris, P.C. and Irwin, G.R. (1965). On cracks in rectilinearly anisotropic bodies. *International Journal of Fracture Mechanics* **1**, 189–203.

Sollero, P. and Aliabadi, M.H. (1993). Fracture mechanics analysis of anisotropic plates by the boundary element method. *International Journal of Fracture* **64**, 269–284.